Topological Insulating Phases in Two-Dimensional Bismuth-Containing Single Layers Preserved by Hydrogenation

Rafael R. Q. Freitas, R. Rivelino, F. de Brito Mota, C. M. C. de Castilho, Anelia Kakanakova-Georgieva and Gueorgui Kostov Gueorguiev

Original Publication:

Rafael R. Q. Freitas, R. Rivelino, F. de Brito Mota, C. M. C. de Castilho, Anelia Kakanakova-Georgieva and Gueorgui Kostov Gueorguiev, Topological Insulating Phases in Two-Dimensional Bismuth-Containing Single Layers Preserved by Hydrogenation, 2015, The Journal of Physical Chemistry C, (119), 41, 23599-23606.
http://dx.doi.org/10.1021/acs.jpcc.5b07961

Topological Insulating Phases in Two-Dimensional Bismuth-Containing Single Layers Preserved by Hydrogenation

R. R. Q. Freitas[†§‡], R. Rivelino*[†], F. de Brito Mota[§†], C. M. C. de Castilho*[§¥],

[†] Instituto de Física, Universidade Federal da Bahia, 40170-115 Salvador, Bahia, Brazil.

[§] Grupo de Física de Superfícies e Materiais, Instituto de Física, Universidade Federal da Bahia, Campus Universitário da Federação, 40170-115 Salvador, Bahia, Brazil.

[¥] Instituto Nacional de Ciência e Tecnologia em Energia e Ambiente (CIENAM) INCT-E&A, Universidade Federal da Bahia, 40170-280 Salvador, Bahia, Brazil.

A. Kakanakova-Georgieva[‡], G. K. Gueorguiev[‡]

[‡] Department of Physics, Chemistry and Biology (IFM), Linköping University, 581 83 Linköping, Sweden

ABSTRACT:

Two-dimensional (2D) binary XBi compounds, where X belongs to group-III elements (B, Al, Ga, and In), in a buckled honeycomb structure may originate sizable-gap Z_2 topological insulators (TIs). These are characterized by exhibiting single band inversion at the Γ point, as well as nontrivial edge states in their corresponding nanoribbons. By using first-principles calculations, we demonstrate that hydrogenation of XBi single layers leads to distinct and stable crystal structures, which can preserve their topological insulating properties. Moreover, hydrogenation opens a band gap in these new class of 2D Z_2 TIs, with distinct intensities, exhibiting an interesting electronic behavior for viable room-temperature applications of these 2D materials. The nature of the global band gap (direct or indirect) and topological insulating properties depend on the X element type and spatial configuration of the sheet, as well as the applied strain. Our results indicate that the geometric configuration can be crucial to preserve totally the topological characteristics of the hydrogenated sheets. We identify sizable band inversions in the band structure for the relaxed hydrogenated GaBi and InBi in their chairlike configurations, and for hydrogenated BBi and AlBi under strain. Based on these findings, hydrogenation gives rise to a flexible chemical tunability and can preserve the band topology of the pristine XBi phases.

KEYWORDS: Topological insulators, spin-orbit effects, bismuth-based 2D materials, hydrogenation.

The growing interest in layered materials for room-temperature electronic applications has led to considering the introduction of novel two-dimensional (2D) systems.[1,2] In this context, honeycomb homonuclear 2D sheets, such as graphene, i.e., silicene[3], germanene,[4,5] and more recently stanene,[6] all belonging to the carbon group, have been synthesized. Furthermore, in the nitrogen group, phosphorene, arsenene and antimonene,[7-10] have been theoreticall/experimentally considered; being obtained as semiconductors with a high hole mobility. In turn, a single layer of bismuth atoms has recently been found to possess a buckled configuration, exhibiting semiconducting properties with an indirect band gap of 500 meV.[11] This new hexagonal homonuclear 2D material, called bismuthene, may be a valuable low-dimensional thermoelectric material similarly to bulk Bi-containing compounds such as Bi_2Te_3 and BiSb.[11,12]

Indeed, Bi-containing materials have opened new perspective mostly related to topological insulators (TIs).[13-15] One of the main reasons for the quest of 2D semiconductors is their much better resistance, in contrast to that of semimetal graphene, to the unfavorable short channel effects at the scaling limit in field-effect transistors (FET).[16] In this direction, Chuang et al.[15] have suited XBi (X = B, Al, In, Ga, and Tl) bilayers finding that GaBi, InBi, and TlBi exhibit a nontrivial band topology with Z_2 topological invariants, which is induced by spin-orbit coupling (SOC). Moreover, by functionalizing these XBi bilayers, they may become Z_2 inversion-asymmetric TIs,[17-19] exhibiting topological invariant $Z_2 = 1$ and producing remarkable Rashba spin splitting, which can be useful for room-temperature electronic applications.

One of the most accessible ways of tuning the properties of these 2D materials is via hydrogenation processes.[4,5] For example, it has been predicted that both silicene and germanene, when fully-hydrogenated to form silicane and germanane, respectively, give rise to wide-bandgap semiconductors.[20] Similarly, upon hydrogenation, the SiC

honeycomb hetero-sheet and the theoretically predicted 2D stanene undergo dramatic increment in their band gaps (from 2.54 eV to 4.04 eV in the case of SiC and from zero to 0.45 eV in the case of stanene).[21]

In this paper, we investigate the topological insulating nature of fully-hydrogenated 2D XBi (X = B, Al, Ga, and In) hetero-sheets in the spatial configurations of hydrogenated bismuthene, or simply bismuthane, induced by SOC. Our results are also compared to their pristine counterparts of XBi. The calculations are performed by employing density functional theory (DFT) calculations without/with inclusion of SOC corrections.[22-26] We investigate first the equilibrium structures of bismuthane and further three configurations (top, chairlike and boatlike) of the hydrogenated XBi (H-XBi) single layers. Thus, we demonstrate that inclusion of SOC is essential to characterize the band structure and band topology of these low-dimensional materials.

The configurations of the hydrogenated systems were modelled by employing a hexagonal unit cell containing four atoms for the top and chairlike configurations, and eight atoms for the boatlike configuration. The length of the lattice vector ***c*** was set to avoid that the interaction between each 2D sheet and its periodic images. Density-functional calculations were carried out within the Perdew-Burke-Ernzerhof[24] generalized gradient approximation, using the projector-augmented wave (PAW) method,[25] as implemented in the Vienna Ab-Initio Simulation Package (VASP).[22-26] A 700 eV kinetic energy cutoff were employed for a 25×25×1 k-point mesh to sample the 2D Brillouin zone (BZ), and a 500 eV cutoff for a 40×1×1 k-point mesh to sample the BZ of the nanoribbons. For the structural optimization, the atoms were allowed to relax until forces below 0.01 eV/Å. The total energy convergence criteria in both geometry optimizations and electronic structure calculations were set to 10^{-5} eV. Spin-orbit coupling was taken into account by performing fully non-collinear magnetic structure

calculations[26] after obtaining the nonmagnetic ground state of the systems, as implemented in the VASP code.

Before performing the electronic structure characterization for the proposed H-XBi sheets, we have examined the crystal structure, dynamic stability, energetics, and electronic properties of bismuthene, which has theoretically been proposed,[11] and may be an interesting platform to incorporate the group-III elements. Our calculations indicate that bismuthene exhibits a buckled equilibrium structure with a buckling parameter Δ = 1.73 Å and a lattice constant a = 4.34 Å (see Figure 1a and Table 1), in good agreement with the work of Cheng et al.[11] Here, we additionally show that the calculated phonon dispersion (Figure 1b) of a single layer of bismuthene should exhibit a dynamically stable structure. Its band structure obtained without and with SOC is provided in Figure 1c. As reported in Table 1, this system exhibits a band gap of 0.555 eV without SOC and 0.500 eV with SOC, being in good agreement with previous calculations.[11]

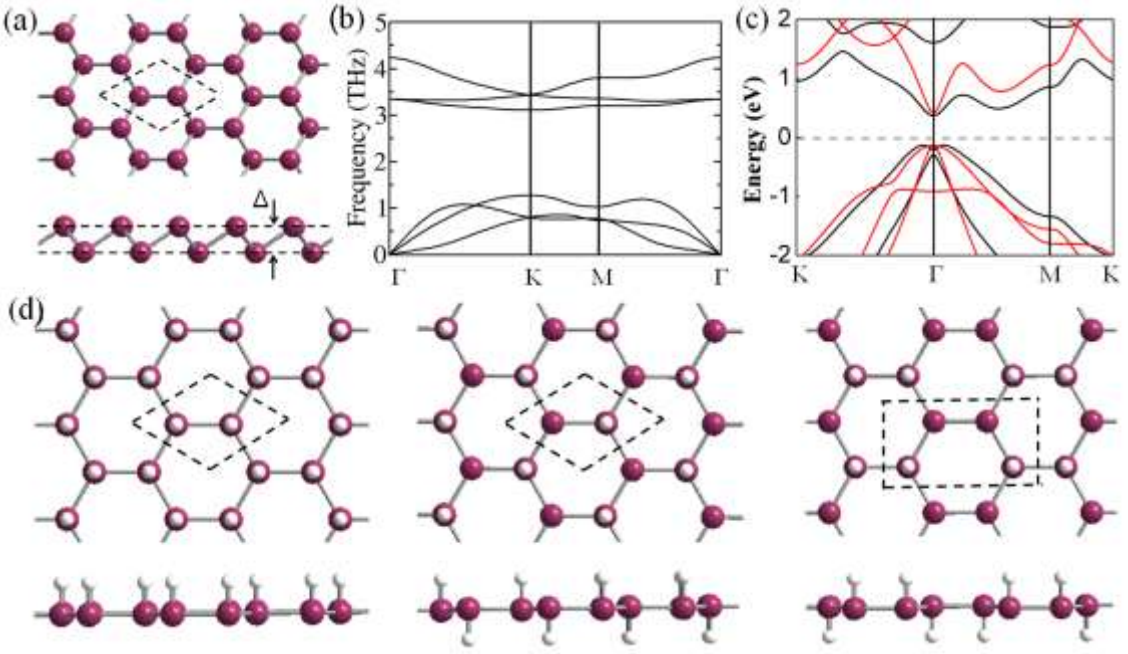

Figure 1. Equilibrium structures of bismuthene and bismuthane: (a) top and side view of an optimized bismuthene sheet; (b) phonon spectrum of a bismuthene sheet; (c) band structure for bismuthene calculated without SOC (red lines) and with SOC (black lines).

(d) Top and side views of the hydrogenated bismuthene (bismuthane) sheets in the top, chairlike, and boatlike configurations, respectively.

As we are interested in the hydrogenation of Bi-containing 2D materials[27], we have considered three different configurations of the fully-hydrogenated bismuthene, which originates the bismuthane sheets. In Figure 1d it is shown the three possible configurations: (i) top, where the H atoms are at the same side of the sheet; (ii) chairlike, characterized by hydrogen atoms alternating on both sides of the sheet; and (iii) boatlike, where the hydrogen atoms are also alternating on both sides of the sheet, but now in pairs. Thus, after relaxation, three isomeric bismuthane sheets are obtained, with the top configuration being a little bit less energetically stable among these three configurations. These structures also serve as starting points for obtaining the fully relaxed H-XBi sheets.

Table 1. Configuration, structural parameters (in Å), energetics and electronic properties (in eV) for bismuthene, the low buckled (LB) XBi sheets, and for their hydrogenated counterparts. Buckling types, lattice constants (a, b), buckling parameter (Δ), cohesive energy per atom ($E_{coh}/_{at}$),[28] adsorption energies per hydrogen atom ($E_{a/H}$),[29] and band gaps (E_g) without and with SOC.

system	*config.*	*buckling*	*a*	*b*	Δ	$E_{coh/at}$	$E_{ads/H}$	E_g	$E_{g\text{-}SOC}$
bismuthene	-	buckled	4.34	-	1.73	2.44	-	0.555[a]	0.500 [b]
	top	planar	5.57	-	0.00	4.15	1.71	0.006[b]	0.707[b]
bismuthane	chairlike	planar	5.51	-	0.08	4.23	1.80	0.026[b]	1.004[b]
	boatlike	planar	5.52	9.56	0.10	4.21	2.62	0.036[b]	0.984[b]
BBi	-	LB	3.89	-	0.51	3.25	-	0.511[a]	0.478[b]
	top	LB	4.16	-	0.14	5.54	2.29	1.900[b]	1.538[b]
H-BBi	chairlike	LB	3.93	-	0.65	5.95	2.70	1.289[a]	0.966[b]
	boatlike	-	3.90	6.76	-	5.91	2.67	1.723[b]	1.616[b]
AlBi	-	LB	4.53	-	0.77	2.56	-	0.751[a]	0.335[b]
H-AlBi	top	LB	4.71	-	0.91	4.59	2.03	0.622[a]	0.181[b]

	chairlike	LB	4.63	-	0.79	4.79	2.22	1.002[a]	0.503[b]
	boatlike	-	4.56	7.90	-	4.79	2.22	1.166[a]	0.915[b]
GaBi	-	LB	4.52	-	0.79	2.31	-	0.107[a]	0.169[b]
	top	LB	4.68	-	1.02	4.19	1.88	0.022[b]	0.368[b]
H-GaBi	chairlike	LB	4.59	-	0.79	4.40	2.09	0.248[a]	0.239[b]
	boatlike	-	4.54	7.88	-	4.39	2.11	0.397[a]	0.037[b]
InBi	-	LB	4.80	-	0.85	2.15	-	0.169[a]	0.175[b]
	top	LB	4.88	-	1.04	3.98	1.83	0.013[b]	0.434[b]
H-InBi	chairlike	LB	4.90	-	0.85	4.12	1.97	0.268[a]	0.271[b]
	boatlike	-	4.81	8.33	-	4.13	2.00	0.320[a]	0.028[b]

[a] Direct band gap. [b] Indirect band gap.

The calculated equilibrium lattice constants of bismuthane are 5.51Å and 5.57Å, respectively, for its top and chairlike configurations (Table 1), while the corresponding buckling parameters are 0.00 (a flat sheet) and 0.08 (a nearly flat sheet). The boatlike configuration is defined by two lattice constants, a = 5.52 Å and b = 9.56 Å with a buckling parameter of 0.10 Å. The Bi-Bi-Bi bond angles are 119.9º and 119.6º, while the H-Bi-Bi bond angles are 88.1º and 88.4º for the boatlike and chairlike sheets, respectively. These angles indicate the formation of a quasi-planar honeycomb structure, upon hydrogenation. We notice that this process occurs in the opposite direction as compared to the transition from graphene to graphane,[21] which tends to be buckled due to the sp^3 hybridization.

In the following, we briefly discuss the energetics of the bismuthane sheets within their equilibrium structures. The cohesive energy per heavy atoms ($E_{coh/at}$)[28] calculated for the three isomeric sheets, indicates that the chairlike (4.23 eV) and boatlike (4.21 eV) sheets are slightly more stable than the top configuration (4.15 eV), as reported in Table 1; although these values are not a guarantee for the thermodynamic stability of these systems. All these three structures are energetically more stable than the equilibrium

buckled sheet of busmuthene (2.44 eV), as well as the pure XBi, with $E_{coh/at}$ varying in the 3.25-2.15 eV range, by increase the atomic number of X. In turn, when the adsorption energy per hydrogen atom ($E_{ads/H}$)[29] is calculated, we obtain that the boatlike configuration presents a higher value (2.62 eV), as compared with the chairlike (1.80 eV) and top configuration (1.71 eV), respectively (see Table 1).

It is more interesting to notice that total hydrogenation dramatically affects the electronic structure of the Bi sheets. The band structure of bismuthane within its chairlike configuration (Figure 2a), as well as within its boatlike configuration (Figure 2b), was calculated without/with SOC in order to investigate the effects on the band-gap energy. As can be seen, in the band structures obtained without SOC there are points where the conduction and valence bands touch each other, for both the chairlike and boatlike bismuthane isomers. This could indicate that these sheets would be essentially gapless materials. However, when SOC is taken into account in the calculations it leads to a large band gap[30] of ~1 eV (1.004 eV for the chairlike and 0.984 eV for the boatlike bismuthane), which is twice larger than the band gap of the bismuthene sheet (see Table 1). More interestingly, bismuthane has been found to exhibit topologically protected edge states[31] for nanoribbons, being a potential candidate for room-temperature applications in spintronics. In this sense, we expect that the effects of hydrogenation can significantly alter the electronic structure of the XBi sheets in the sense of obtaining viable materials, exhibiting nontrivial band topology.

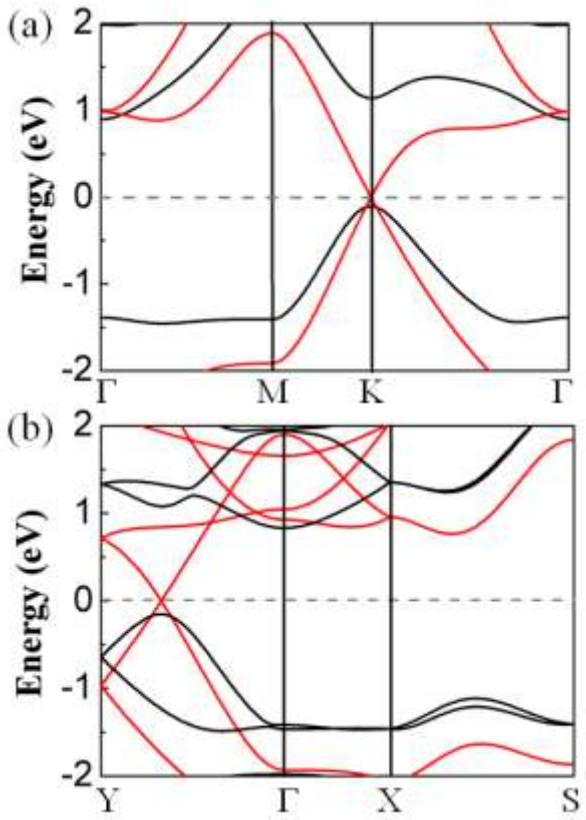

Figure 2. Band structure calculated without SOC (red lines) and with SOC (black lines) for bismuthane: (a) in chairlike and (b) in boatlike configurations.

By analogy with bismuthane (Figure 1d), three different configurations for the fully-hydrogenated XBi (X = B, Al, Ga, and In) hetero-sheets were considered in this work. The dynamic stability of the chairlike configurations of these single layers has been confirmed by phonon calculations.[17] In Figure S1 (see Supporting Information), we display our calculated phonon spectra of two representative cases of XBi and boatlike H-XBi configurations. The optimized structural parameters of the H-XBi hetero-sheets are provided in Table 1. Depending on the group-III element involved, their lattice constants vary in the ranges of 4.16–4.88 Å and 3.93–4.90Å for the top and chairlike configurations, respectively. In the case of the boatlike isomers, the two lattice constants, *a* and *b*, defining the corresponding unit cell, vary in the range of 3.90–4.81 Å and 6.76–8.33 Å, respectively. Moreover, their buckling parameters fall into the ranges of 0.14–1.04 Å and

0.65–0.85Å for the top and the chairlike configurations, respectively. This makes these systems being low buckled sheets, in contrast to the essentially flat sheets of bismuthane (in all the three structures: top, chairlike and boatlike). In the case of all H-XBi, the boatlike configurations exhibit a slightly distorted structure compared with the boatlike bismuthane. Similar distortion also appears in the boatlike configuration of fully-fluorinated boron nitride sheet (FBNF)[32] In principle, significant distortions of this type make difficult to define a buckling parameter in such cases.

The calculated values of the cohesive energies per heavy atom[28] for all H-XBi structures in the different configurations are presented in Table 1. As in the case of bismuthene/bismuthane, these systems are energetically more stable than their pristine counterparts. These results indicate that the energetically similar chairlike and boatlike structures may exhibit advantages in stability when compared to their top counterparts. Also, the adsorption energies of hydrogen atoms in the case of the chairlike (1.97–2.70 eV) and boatlike (2.0–2.67 eV) H-XBi structures (for all group-III elements) are larger than the adsorption energies of their top counterparts (1.83–2.29 eV). This may attribute an additional experimental feasibility to all chairlike and probably boatlike H-XBi configurations, although these latter configurations are slightly distorted as compared to the most common boatlike structures, such as that occurring for graphane. As we will discuss in the following, this structural deformation may affect the nontrivial band topology of the hydrogenated XBi single layers.

For completeness of our study concerning the topological characteristics of the H-XBi sheets, we also report in Table 1 the effect of SOC on the calculated band gaps of the three configurations of H-XBi. The band gap values for the chairlike and boatlike configurations calculated without SOC differ significantly, being larger for H-BBi (1.29 and 1.72 eV, respectively) and H-AlBi (1.00 and 1.17 eV, respectively). Contrastingly,

H-GaBi (0.25 and 0.40 eV) and H-InBi (0.27 and 0.32 eV) exhibit essentially smaller band gap values (for the chairlike and boatlike configurations, respectively). In all these cases, the band gap type is direct, without SOC, with the exception of the boatlike H-BBi sheet. However, if SOC is turned on, the band gap values are reduced, with the exception of H-InBi, which appears to exhibit a small increase in the band gap of 3 meV. Now, the band gaps read 0.97 and 1.62 eV for H-BBi, and 0.50 eV and 0.92 eV for H-AlBi, in their chairlike and boatlike configurations, respectively. It is important, however, to emphasize that when SOC is taken into account in the calculations, in all cases the band gap type becomes indirect. Interestingly, in the case of the chairlike configurations, it is possible to observe a clear breaking in the band degeneracy at the Γ point (see Figure S2 in the SI), forming a Rashba-like dispersion.[17,33] This spin splitting is also very similarly to what occurs for the non-hydrogenated XBi sheets. Furthermore, the Rashba effect dramatically decreases the band gap of the boatlike H-GaBi and H-InBi configurations, in comparison to their chairlike counterparts, due to a stronger spin-orbit effect in these structures.

Based on the analysis of the energetics for the fully-hydrogenated XBi sheets, we have calculated the band structures of H-XBi within the chairlike and boatlike configurations. Yet, the band gap values and nature (direct or indirect) for all three configurations are summarized in Table 1. Here, as we are interested in nontrivial topological properties, we report only the band structure of H-GaBi within the chairlike and boatlike configurations in more details (see Figures S2 and S3 for additional results). In order to investigate nontrivial 2D Z_2 TI phases for H-XBi, we have calculated the band structure without and with SOC, by projecting the contribution of the s-orbitals in the wave function, associated with valence and conduction band extrema at the center of the BZ. As in the case of the pristine XBi sheets, we identify typical band inversions[14] only in the band structures of H-GaBi and H-InBi. An example is shown in Figure 3, where

the band structures for the chairlike and boatlike H-GaBi sheets are calculated without SOC (left panels) and with SOC (right panels). We stress that the inclusion of SOC is essential for obtaining an accurate description of the electronic structure of all these systems, exhibiting the Rashba spin splitting near the Fermi level (see Figures S2, S3 and Figure 3). In particular, band inversions are only observed in the band structures calculated with SOC.

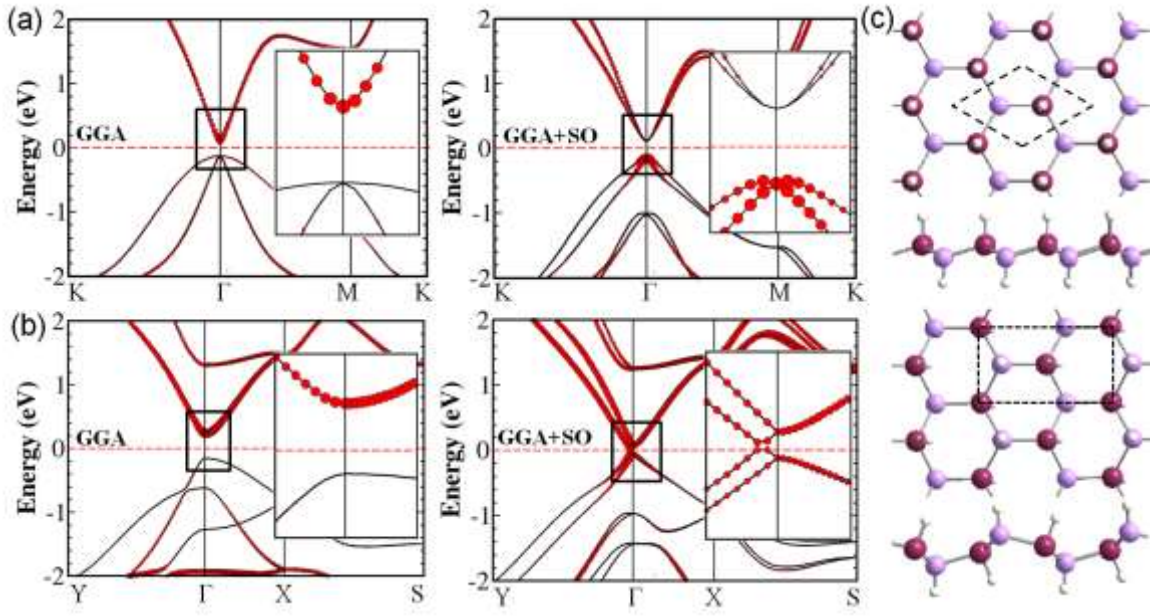

Figure 3. Band structure calculated without SOC (left panels) and with SOC (right panels) for (a) H-GaBi in the chairlike configuration and (b) H-GaBi in a boatlike configuration. Sizes of red circles are proportional to the contribution of the s-orbital in the wave function (see the insets for clarity) and red dashed lines indicate the Fermi level. (c) Relaxed structures of the chairlike (top) and boatlike (botom) sheets (black dashed lines indicate the unit cells).

It is worth to observe that hydrogenation seems to preserve totally band inversions observed in the cases of H-GaBi and H-InBi, especially in their chairlike structures (see Figure 3a for H-GaBi and Figure S2c for H-InBi), which do not exhibit significant structural deformations compared to the initial symmetry of the unit cells. On the other hand, in the case of the boatlike H-GaBi (Figure 3b) and H-InBi (Figure S3c) structures, which are significantly deformed after relaxation, there is only a partial contribution of

the s-orbitals in the wave function, which is also present at the bottom of the conduction band. Interestingly, the nature of the band inversions observed in chairlike H-XBi is similar to that of their corresponding pristine XBi sheets (X = Ga and In). Thus, these results indicate that hydrogenation appears to preserve the topological insulating phases of XBi, and may affect the nontrivial band topology of the H-XBi hetero-sheets, depending on their spatial configurations. We recall that this topological feature is markedly different from other 2D TIs, such as a single bilayer tin film, for which hydrogenation leads to a trivial insulator.[34,35] However, it is still necessary determining nontrivial topological edge states in the ribbons of these H-XBi sheets to classify them as 2D Z_2 TIs.

As an appealing case, since indium is not a toxic hazard and is of considerable industrial interest, we have examined more deeply the topological properties of chairlike and boatlike H-InBi (see band structures in Figures S2 and S3). As can be noticed by the band inversions, apparently the nature of the topological insulating properties may be affected by the fact that these relaxed boatlike structures are significantly distorted. This is more evident when the atomic number increases for the group-III element, in comparison to other more symmetric boatlike structures. To evaluate the nontrivial edge states in these structures, we have considered large (~9 nm) zigzag nanoribbons of H-InBi (chairlike and boatlike) within their relaxed lattice constants, as displayed in Figure 4.

From the calculated band structures of the nanoribbons, we found two different topologically protected edge states in the chairlike 22-ZNR (Figure 4a), and in the boatlike 22-ZNR (Figure 4b). It is seen that these edge states form bands connecting valence and conduction bands and linearly cross the X symmetry point in the BZ. Thus, both configurations exhibit two Dirac cones split owing to the asymmetric edges. As

emphasized in Figure 4, the contribution from the Bi-terminating edges (violet spheres) are indicated by blue circles, while the In-terminating edges (orange spheres) are indicated by red circles in the band structures. From Γ to X point, the edge bands are described by an odd number of crossings over the Fermi level, indicating that these systems are possibly 2D Z_2 TIs, in both the pure phase[14] and upon hydrogenation.

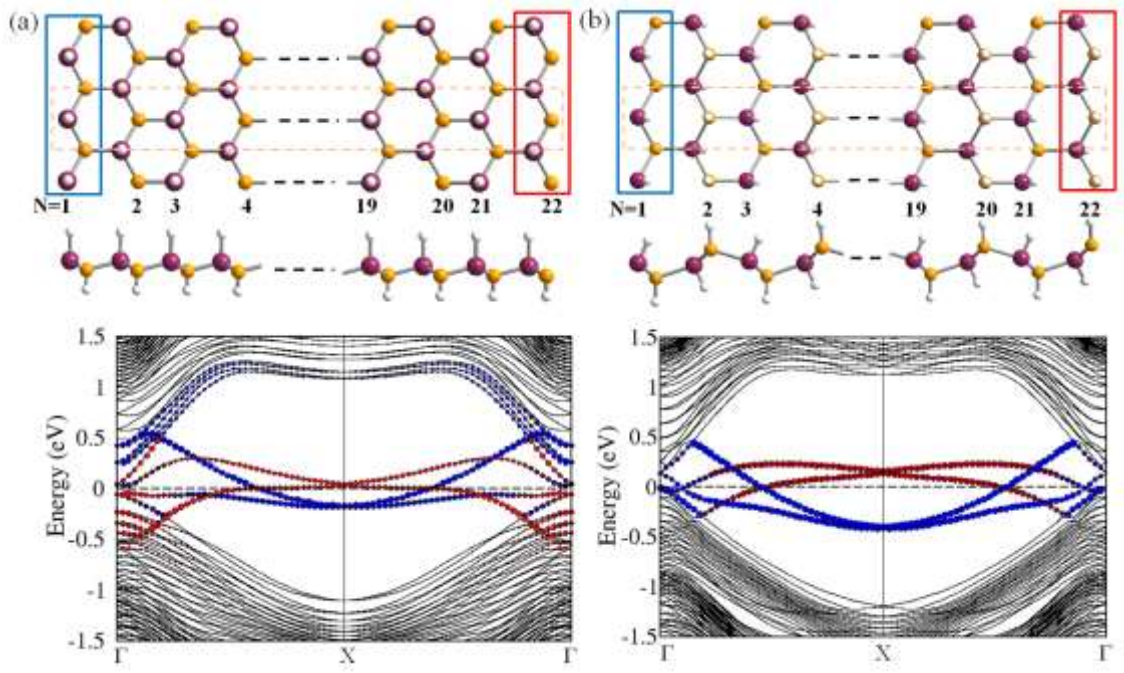

Figure 4. Views of the spatial structures (top) and band structures (bottom) of H-InBi nanoribbons with zigzag edges (22-ZNR) for the chairlike (a) and boatlike (b) configurations. Orbital contributions from the Bi-terminating edges (blue rectangles) are indicated by blue circles, while the In-terminating edges (red rectangles) are indicated by red circles. Sizes of the circles are proportional to the orbital contribution of the edge atoms in the wave function and the Fermi level is set at zero energy.

As a complement to the topological analysis of the H-XBi sheets, in Figure 5 we have calculated the band-inversion strength (BIS), as defined in References,[14,36] for both pure and hydrogenated XBi sheets. This quantity gives an indication of how a buckled system is far from a topological critical point and has been useful to classify Bi-containing 2D TIs, which possess a nontrivial Z_2 topological invariant.[36] First, we have determined the BIS at the Γ point for the fully-relaxed chairlike H-XBi sheets and compared their values with the ones of pristine XBi sheets. As in the case of XBi (Figure 5a), we notice

that only for H-GaBi and H-InBi, the BIS values are positive, which indicate band inversions in the presence of SOC. On the contrary, for H-BBi and H-AlBi the BIS values are negative, indicating that these systems, at equilibrium, are trivial insulators, owing to the small SOC in B and Al atoms. These results demonstrate that hydrogenation of XBi single layers leads to a topological behavior similar to that observed for pristine XBi, indicating that this chemical change may preserve the trivial and nontrivial band topology of these 2D systems.

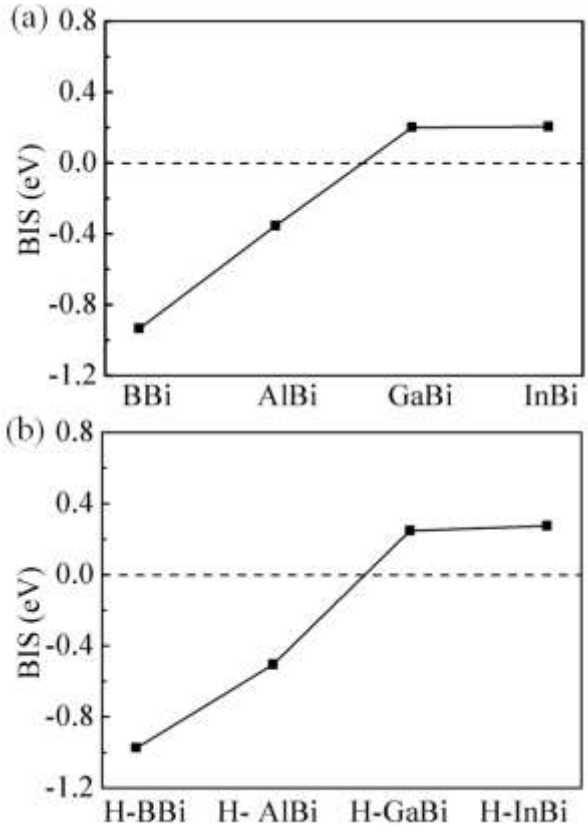

Figure 5. Band-inversion strength (BIS) at the Γ point for (a) pristine XBi hetero-sheets and (b) hydrogenated XBi hetero-sheets in their chairlike configurations.

In addition to the analysis of the BIS for the equilibrium structures, we have investigated the effect of strain in the H-XBi sheets, also compared to the pristine XBi counterparts. As is known, strain can lead to topological phase transitions in Bi, Sb, and XBi bilayers.[14,15] Hence, we have obtained both crystal and electronic structures at each

value of the lattice constant by relaxing the atomic positions in the buckled state. In Figure 6, we display the BIS values as a function of strain for the XBi and H-XBi sheets. Again, we notice that the positive BIS values indicate topologically nontrivial phases, whereas negative BIS values are trivial insulators. Now, similarly to the case of XBi, H-BBi and H-AlBi may reach a condition of TIs under high strain. On the other hand, H-GaBi and H-InBi can be transformed into trivial phases under negative strain lesser than –3.5% (Figure 6b). These results also confirm that the overall topological behavior of XBi appears to be preserved upon hydrogenation.

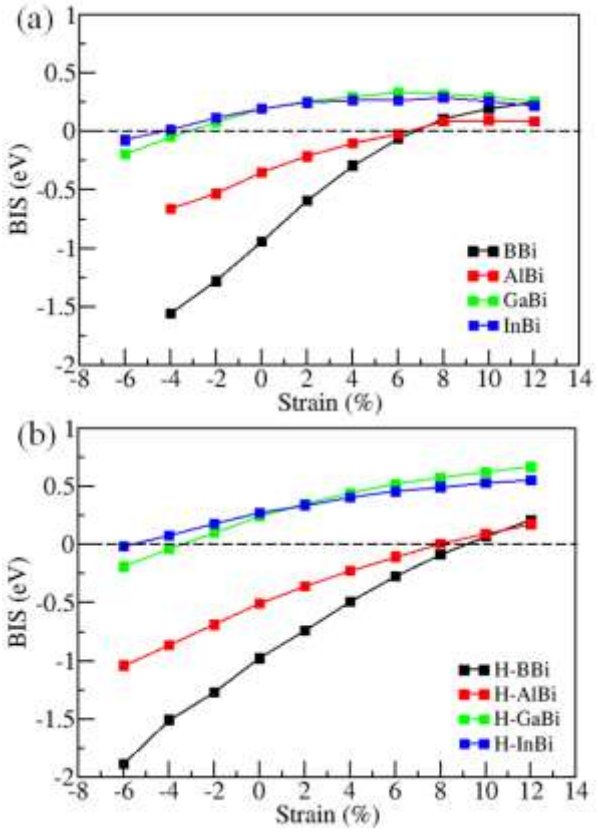

Figure 6. Band-inversion strength (BIS) at the Γ point for (a) pristine XBi hetero-sheets and (b) hydrogenated XBi hetero-sheets in their chairlike configurations as a function of strain.

In summary, first-principles calculations were employed to investigate the crystal structure, electronic properties and topological insulating characteristics of fully-

hydrogenated 2D XBi (X = B, Al, In, and Ga) hetero-sheets. Our calculations were also compared with bismuthane in three different configurations (top, chairlike and boatlike). Our results, in all cases, have indicated that the cohesive energies of the chairlike and boatlike configurations are very similar for these systems, which may be more stable than the top configuration. For pristine bismuthene, we have demonstrated that when SOC is taken into account it results in the breaking of the valence-band energy degeneracy at the Γ point, leading to an indirect band gap semiconductor with 0.50 eV. Upon hydrogenation of busmuthene, SOC leads to a significant band gap of ~1 eV, being indirect in all considered configurations.

In the case of the XBi hetero-sheets, hydrogenation opens a band gap in all cases, with distinct intensities, exhibiting an interesting semiconducting behavior for viable room-temperature applications. Inclusion of SOC affects the nature of the band gap (direct or indirect), displays a Rashba-type spin spliting, and reveals topological insulating properties, which depend on the group-III element, strain and spatial configuration of the hydrogenated sheet. For instance, a clear band inversion occurs only for H-GaBi and H-InBi in their relaxed charlike configurations, while it is not so clear in the boatlike configurations, mainly owing to their spatial deformation, after relaxation. Of course, this may affect the band topology of the 2D TIs, as indicated by the edges estates of chairlike and boatlike nanoribbons. However, in the case of the chairlike configuration, we have demonstrated that hydrogenation can preserve the topological insulating characteristic of the pure XBi phases, even under strain.

These present theoretical results represent significant advances for the understanding of Bi-containing 2D TIs with Z_2 topological invariant. In this sense, we expect to stimulate further experimental works to synthesize, characterize, as well as to

utilize these new class of low-dimensional materials for fundamental studies and practical applications.

ASSOCIATED CONTENTS

Supporting Information

Calculated phonon spectra of GaBi and boatlike H-GaBi, and band structures of H-XBi (X = B, Al, and In). The Supporting Information is available free of charge on the ACS Publications website at DOI: xxxxxxxxxx.

AUTHOR INFORMATION

Corresponding Authors

*E-mail: rivelino@ufba.br. Phone: +55 71 3283-6640. Fax: +55 71 3283-6606.

*E-mail: caio@ufba.br. Phone: +55 71 3283-6640.

Notes

The authors declare no competing financial interest.

ACKNOWLEDGMENTS

The authors gratefully acknowledge partial financial support for this work by the Swedish Research Council (VR) through Swedish Research links Project 348-2014-4249. G.K.G. and A. K. G. gratefully acknowledge support by the Linköping Linnaeus Initiative for Novel Functionalized Materials (LiLi-NFM, VR). G. K. G. acknowledges support by the Swedish Foundation for Strategic Research (SSF) Synergy Grant #RMA11-0029 on Functional Carbides and Advanced Surface Engineering (FUNCASE). R.R., C.M.C.deC., and F.deB.M. acknowledge Conselho Nacional de Desenvolvimento Científico e Tecnológico (CNPq) and Fundação de Amparo à Pesquisa do Estado da Bahia (FAPESB) for partial support. R.R.Q.F. acknowledges the support by Coordenação de

Aperfeiçoamento de Pessoal de Nível Superior (CAPES). We acknowledge the fruitful discussions with Dr. S. Cunha during the early stages of this work.

References

1. Xu, M. S.; Liang, T.; Shi, M. M.; Chen, H. Z. Graphene-Like Two-Dimensional Materials. *Chem. Rev.* **2013,** *113*, 3766-3798.

2. Butler, S. Z.; Hollen, S. M.; Cao, L. Y.; Cui, Y.; Gupta, J. A.; Gutierrez, H. R.; Heinz, T. F.; Hong, S. S.; Huang, J. X.; Ismach, A. F.; et al. Progress, Challenges, and Opportunities in Two-Dimensional Materials Beyond Graphene. *ACS Nano* **2013,** *7*, 2898-2926.

3.Vogt, P.; De Padova, P.; Quaresima, C.; Avila, J.; Frantzeskakis, E.; Asensio, M. C.; Resta, A.; Ealet, B.; Lay, G. L. Silicene: Compelling Experimental Evidence for Graphenelike Two-Dimensional Silicon. *Phys. Rev. Lett.* **2012,** *108*, 155501.

4. Davila, M. E.; Xian, L.; Cahangirov, S.; Rubio, A.; Lay, G. L. Germanene: A Novel Two-Dimensional Germanium Allotrope Akin to Graphene and Silicene. *New J. Phys.* **2014,** *16*, 095002.

5. Bianco, E.; Butler, S.; Jiang, S. S.; Restrepo, O. D.; Windl, W.; Goldberger, J. E. Stability and Exfoliation of Germanane: A Germanium Graphane Analogue. *ACS Nano* **2013,** *7*, 4414-4421.

6. Zhu, F.; Chen, W.; Xu, Y.; Gao, C.; Guan, D.; Liu, C.; Qian, D.; Zhang, S.-C.; Jia, J. Epitaxial Growth of Two-Dimensional Stanene. *Nature Mater*. **2015**, DOI: 10.1038/NMAT4384.

7. Liu, H.; Neal, A. T.; Zhu, Z.; Luo, Z.; Xu, X. F.; Tomanek, D.; Ye, P. D. D. Phosphorene: An Unexplored 2D Semiconductor with a High Hole Mobility. *ACS Nano* **2014,** *8*, 4033-4041.

8. Zhang, S. L.; Yan, Z.; Li, Y. F.; Chen, Z. F.; Zeng, H. B. Atomically Thin Arsenene and Antimonene: Semimetal-Semiconductor and Indirect-Direct Band-Gap Transitions. *Angew. Chem. Int. Ed.* **2015,** *54*, 3112-3115.

9. Guan, J.; Zhu, Z.; Tomanek, D. Tiling Phosphorene. *ACS Nano* **2014,** *8*, 12763-12768.

10. Woomer, A. H.; Farnsworth, T. W.; Hu, J.; Wells, R. A., Donley, C. L.; Warren, S. C. Phosphorene: Synthesis, Scale-up, and Quantitative Optical Spectroscopy. *ACS Nano* **2015**, DOI: 10.1021/acsnano.5b02599.

11. Cheng, L.; Liu, H. J.; Tan, X. J.; Zhang, J.; Wei, J.; Lv, H. Y.; Shi, J.; Tang, X. F. Thermoelectric Properties of a Monolayer Bismuth. *J. Phys. Chem. C* **2014,** *118*, 904-910.

12. Shi, H.; Parker, D.; Du, M.-H.; Singh, D. J. Connecting Thermoelectric Performance and Topological-Insulator Behavior: Bi_2Te_3 and Bi_2Te_2Se from First Principles. *Phys. Rev. Appl*. **2015**, *3*, 014004.

13. Huang, Z. Q.; Chuang, F. C.; Hsu, C. H.; Liu, Y. T.; Chang, H. R.; Lin, H.; Bansil, A. Nontrivial Topological Electronic Structures in a Single Bi(111) Bilayer on Different Substrates: A First-Principles Study. *Phys. Rev. B* **2013,** *88*, 165301.

14. Chuang, F. C.; Yao, L. Z.; Huang, Z. Q.; Liu, Y. T.; Hsu, C. H.; Das, T.; Lin, H.; Bansil, A. Prediction of Large-Gap Two-Dimensional Topological Insulators Consisting of Bilayers of Group III Elements with Bi. *Nano Lett.* **2014,** *14*, 2505-2508.

15. Chen, L.; Wang, Z. F.; Liu, F. Robustness of Two-Dimensional Topological Insulator States in Bilayer Bismuth against Strain and Electrical Field. *Phys. Rev. B* **2013,** *87*, 235420.

16. Fang, H.; Chuang, S.; Chang, T. C.; Takei, K.; Takahashi, T.; Javey, A. High-Performance Single Layered WSe_2 p-FETs with Chemically Doped Contacts. *Nano Lett.*

2012, *12*, 3788-3792.

17. Ma, Y.; Li, X.; Kou, L.; Yan, B.; Niu, C.; Dai, Y.; Heine, T. Two-Dimensional Inversion-Asymmetric Topological Insulators in Functionalized III-Bi Bilayers. *Phys. Rev. B* **2015**, *91*, 235306.

18. Ma, Y.; Dai, Y.; Kou, L.; Frauenheim, T.; Heine, T. Robust Two-Dimensional Topological Insulators in Methyl-Functionalized Bismuth, Antimony and Lead Bilayer Films. *Nano Lett*. **2015**, *15*, 1083–1089.

19. Ma, Y.; Dai, Y.; Kou, L.; Du, A.; Heine, T. Group 14 Element Based Noncentrosymmetric Quantum Spin Hall Insulators with Large Bulk Gap. *Nano Res.* **2015**,

DOI 10.1007/s12274-015-0842-7.

20. Houssa, M.; Scalise, E.; Sankaran, K.; Pourtois, G.; Afanas'ev, V. V.; Stesmans, A. Electronic Properties of Hydrogenated Silicene and Germanene. *Appl. Phys. Lett.* **2011,** *98*, 223107.

21. Garcia, J. C.; de Lima, D. B.; Assali, L. V. C.; Justo, J. F. Group IV Graphene- and Graphane-Like Nanosheets. *J. Phys. Chem. C* **2011,** *115*, 13242-13246.

22. Kresse, G.; Hafner, J. Ab Initio Molecular-Dynamics for Liquid-Metals. *Phys. Rev. B* **1993,** *47*, 558-561.

23 Kresse, G.; Furthmuller, J. Efficient Iterative Schemes for Ab Initio Total-Energy Calculations Using a Plane-Wave Basis Set. *Phys. Rev. B* **1996,** *54*, 11169-11186.

24. Perdew, J. P.; Burke, K.; Ernzerhof, M. Generalized Gradient Approximation Made Simple. *Phys. Rev. Lett,* **1996,** *77*, 3865-3868.

25. Kresse, G.; Joubert, D. From Ultrasoft Pseudopotentials to the Projector Augmented-Wave Method. *Phys. Rev. B* **1999,** *59*, 1758-1775.

26. Hobbs. D.; Kresse, G.; Hafner, J. Fully Unconstrained Noncollinear Magnetism

within the Projector Augmented-Wave Method. *Phys. Rev. B* **2000**, *62*, 1156.

27. Song, Z.; Liu, C.-C.; Yang, J.; Han, J.; Ye, M.; Fu, B. Yang, Y.; Niu, Q.; Lu, J.; Yao, Y. Quantum Spin Hall Insulators and Quantum Valley Hall Insulators of BiX/SbX (X=H, F, Cl and Br) Monolayers with a Record Bulk Band Gap. *NPG Asia Mat.* **2014**, *6*, e147.

28. Cohesive energy per atom (without including hydrogen atom) is defined as $E_{coh/at} = -\frac{1}{N}(E_{total} - n_X E_X - n_{Bi} E_{Bi} - n_H E_H)$, where E_X, E_{Bi} and E_H are the total energies of the isolated atoms and E_{total} is the total energy per unit cell of the compound. The coefficients n_X, n_{Bi} and n_H are the corresponding numbers of atoms, X, Bi and H, present in the unit cell, while $N = n_X + n_{Bi}$ is the total number of heavy atoms.

29. Adsorption energy per hydrogen atoms is calculated according to the formula $E_{ads/H} = -(E_{HXBi} - E_{XBi} - n_H E_H)$, where E_{HXBi}, E_{XBi}, E_H, n_H are, respectively, the total energy of the hydrogenated system, the total energy of the pure counterparts, the energy of an isolated hydrogen atom in its spin-polarized ground state, and the number of adsorbed hydrogen atoms.

30. Keum, D. H.; Cho, S.; Kim, J. H.; Choe, D. H.; Sung, H. J.; Kan, M.; Kang, H.; Hwang, J. Y.; Kim, S. W.; Yang, H.; et al. Bandgap Opening in Few-Layered Monoclinic $MoTe_2$. *Nature Phys.* **2015,** *11*, 482-486.

31. Hsu, C.-H.; Huang, Z.-Q.; Chuang, F.-C.; Kuo, C.-C.; Liu, Y.-T.; Lin, H.; Bansil. A. The Nontrivial Electronic Structure of Bi/Sb Honeycombs on SiC(0001). *New J. Phys*. **2015**, *17*, 025005.

32. Noor-A-Alam, M.; Kim, H. J.; Shin, Y. H. Dipolar Polarization and Piezoelectricity of a Hexagonal Boron Nitride Sheet Decorated with Hydrogen and Fluorine. *Phys. Chem. Chem. Phys.* **2014,** *16*, 6575-6582.

33. Ishizaka, K.; Bahramy, M. S.; Murakawa, H.; Sakano, M.; Shimojima, T.; Sonobe, T.; Koizumi, K. ; Shin, S. ; Miyahara, H. ; Kimura, A.; et al. Giant Rashba-type Spin

Splitting in Bulk BiTeI. *Nature Mater.* **2011**, *10*, 521-526.

34. Xu, Y.; Yan, B. H.; Zhang, H. J.; Wang, J.; Xu, G.; Tang, P. Z.; Duan, W. H.; Zhang, S. C. Large-Gap Quantum Spin Hall Insulators in Tin Films. *Phys. Rev. Lett.* **2013,** *111*, 136804.

35. Chou, B.-H., Huang, Z.-Q., Hsu, C.-H.; Chuang, F.-C.; Yu-Tzu Liu, Y.-T.; Lin, H.; Bansil, A. Hydrogenated Ultra-Thin Tin Films Predicted as Two-Dimensional Topological Insulators. *New J. Phys.* **2014,** *16*, 115008.

36. Huang, H. Q.; Liu, J. P.; Duan, W. H. Nontrivial Z(2) Topology in Bismuth-Based III-V Compounds. *Phys. Rev. B* **2014,** *90*, 195105.

TOC

Abstract graphic